

Robust Face Recognition under Varying Light Based on 3D Recovery

Guan Yang Fei Xue GuoCan Feng¹

Center of Computer Vision, School of
Mathematics and Computing, Sun Yat-sen
University, Guangzhou, China 510275

mcsfgc@mail.sysu.edu.cn

Ching Y Suen

Centre for Pattern Recognition and Machine
Intelligence, Concordia University, Montreal,
Canada, H3G 1M8

parmidir@cenparmi.concordia.ca

ABSTRACT

This paper addresses face recognition under varying light via 3D reconstruction based on the techniques of shape from shading (SFS). First, we improve the geometric-based SFS by introducing the integrability constraint as one of the regular terms. This operation preserves the local curvedness of the recovered surface. Second, we propose a novel method to investigate human face recognition in the illumination varying case using local topographic information, such as curvedness and shape index extracted from intensity images by SFS algorithms. The experimental results have shown that the curvedness and shape index are suitable for representing 3D local features, and also it is insensitive to light variations since only 3D information is involved. Compared with typical face recognition approaches based on principal component analysis (PCA) plus linear discriminant analysis (LDA), the proposed method has demonstrated a better performance. This implies local topological properties are effective attributes for face recognition under light variations

Keywords

Face recognition, shape from shading (SFS), surface normal field, curvedness histogram, shape index

1. INTRODUCTION

Face recognition technique has been studied for decades because of its wide applications such as recognition and verification of personal identity, public safety, etc [Zha03]. However, face recognition under illumination variation is still a challenging task. According to the report of FERET test, the recognition error will rise rapidly with light variations for some of the existing recognition systems [Phi00]. Recent FRVT evaluation report also showed that most of the algorithms are still sensitive to outdoor light variations [Phi03]. Nowadays, more researchers have focused on challenging issues arising from illumination, pose and facial expressions. Illumination variation is one of most difficult problems and has received much attention [Tur91, Bel97, Mog00, Sha01, Liu06, Zha99, Zha00a, Zha00b, Wor01]. As far as we know, the algorithms of face recognition for overcoming illumination variation can be divided into two categories: statistical-based and model-based. In the former category, the invariant features or parameters to light variation are extracted to present the normalized

object through statistical analysis. Typical algorithms include Eigenfaces[Tur91], Fisherfaces[Bel97] and Bayesian-based [Mog00] etc. The latter category is under the assumption that a human face is a Lambertian surface. Under the assumption, new 2D light normalizing appearance images are synthesized to be applied in recognition stage. The illumination cone-based [Geo01] and quotient image [Sha01, Liu06] belong to this category. The illumination cone theory tells us the set of images of any object in a fixed pose, but under all light conditions, is a convex cone in image space [Geo01]. According to this rule, one face image can be expressed by the linear representation of other 3 images under independent light. The face recognition based on the illumination cone can handle light variations quite well. However, at least 3 images under different light directions are required in the training stage in this algorithm in order to obtain the feature representation. In quotient image algorithms, 3D face models are required, while most algorithms adopted the same generic 3D mask [Liu06]. So errors will be introduced due to the depth differences among the subjects.

¹ Corresponding author, Guo Can Feng, is with the Center of Computer Vision, School of Mathematics and Computing, Sun Yat-sen University, Guangzhou, China, E-mail: mcsfgc@mail.sysu.edu.cn. This work is partially supported by the National Natural Science Foundation of China under grant No. 60675007 and the Education Ministry of China under key grant No. 104145

Like the simulating visual ability of human beings, SFS is one of the useful computer vision methods concerned with recovering surface topography from intensity pictures. Although it developed quickly, one of the biggest limitations in most SFS algorithms is that they fail to provide an accurate the shape of surface. This is due to the loss of a large amount of height information when 2D pictures are projected from 3D objects. In essence, SFS is a mapping from 2D space to 3D space, so it is an ill-posed problem. However, the SFS problem has attracted many researchers and made good progress. Generally speaking, SFS techniques can be divided into four types according to the attached constraint [Zha99]: minimization, propagation, localization and linearization approaches. Minimization approach was first presented by Ikeuchi and Horn [Hor70, Ike81], who introduced the brightness and smoothness constraints. Frankot and Chellappa [Fra88] enforced integrability in the energy function in order to recover integrable surfaces. Propagation methods propagate the surface shape from a set of particular points(e.g., singular points) to the whole image. Bichsel and Pentland [Bic92] presented an algorithm as minimum downhill principle, which requires prior knowledge of the heights of singular points. Rouy and Tourin's approach[Rou92] is based on Hamilton-Jacobi-Bellman equation and viscosity solution theories which provide conditions for the existence of both continuous and smooth solutions. Prados and Faugeras [Pra03] developed the notion of viscosity solutions for SFS and proposed generic SFS for both orthographic and perspective projection. Lee and Rosenfeld [Lee85] computed the solution on the assumption that the surface is locally spherical. Linear methods compute the solution based on the linearization of the reflectance map. Tsai and Shahis method [Tsa94] is one of the typical linear SFS algorithms.

Since most algorithms cannot derive accurate shapes, many papers focused on surface reconstruction rather than recognition. Up to now, few papers explored object recognition using the SFS technique. Zhao and Chellappa [Zha00a,Zha00b] presented a model-based bilateral symmetric SFS algorithm, which improves the performance of a face recognition system in handling illumination variations via image synthesis. But in practice, the symmetry assumption limits its application. More recently, Worthington and Hancock and Worthington [Wor01] presented a geometric-based SFS recovering accurate surface normal fields, and used normal fields for object recognition in handling variations due to pose. However, they did not consider the surface integrability constraint, which brings the shape index to be an invariant feature to light variations for real images.

Following Worthington and Hancock's idea, the extra integrability constraint in the radiance equation is included in this paper. Then, along with the 3D surface normal field constructed by the proposed algorithm, curvedness and shape index are developed and applied in a face recognition system. The experimental results have shown the proposed method works well and is robust in handling light variations.

The rest of this paper is organized as follows: following Worthington and Hancock's geometric-based SFS algorithm, the integrability constraint as a new regular term is introduced to improve the robustness of 3D reconstruction. The derivation of 3D reconstruction is introduced in section 2. Then we explore three strategies of face recognition based on the similarity of surface normal fields in section 3. The experimental results for 3D recovery and face recognition are demonstrated in section 4. Finally, we draw some conclusions in Section 5.

2. NORMAL FIELD RECOVERY BASED ON SFS

Our SFS algorithm is following Worthington and Hancock's Geometric-based SFS [Wor99] with an extra improvement in the integrability regular term, which preserves fine surface normal fields. These normal fields form the groundwork of recognition strategies in the next section.

A. Reflect Cone

Under Lambertian assumption, the image intensity is determined by cosine value of the angle between light direction and surface normal. That means the image irradiance equation defines a cone of possible surface normal direction. The axis of this cone is in the direction of light and the opening angle is determined by corresponding brightness. With this observation, a hard constraint to satisfy the image irradiance equation is proposed, and it makes surface normal fall on this cone.

To be formal, for the surface $Z=Z(x,y)$, let us denote $n_{i,j}$ the unit normal of the surface Z at the lattice position (i, j) and S a unit vector of light direction. Then the corresponding brightness $E_{i,j}$ is determined by:

$$E_{i,j} = \rho n_{i,j} \cdot S \quad (1)$$

where brightness $E_{i,j}$ has been normalized (here assume *albedo* ρ as 1). So the reflect cone has the opening angle $\phi = \arccos E_{i,j}$. In order to define the reflect cone correctly, we need to determine the light direction reliably. There are many related

algorithms [Zhe91, Lee85]. In our experiments, Lee and Rosenfeld's method [Lee85], for its simplicity and good results, is used here as a pretreatment to estimate the light direction.

B. Additional Constraints

In the classical minimization approach, Horn and Brooks [Hor81] first used the following energy function with the smooth constraint:

$$I = \iint (E(x, y) - (n \cdot S))^2 + \lambda \left(\left\| \frac{\partial n}{\partial x} \right\|^2 + \left\| \frac{\partial n}{\partial y} \right\|^2 \right) dx dy \quad (2)$$

where n is the surface normal. The first term is known as brightness constraint and it facilitates satisfaction of the image reflection function. The second expression is a regular term which imposes a smoothness constraint on the recovered surface normal. In our proposed algorithm, the brightness constraint is treated as a hard constraint to ensure the data-closeness between the image intensity E and the reflectance function $n \cdot S$. Usually, there are four kinds of constraints [Zha99]:

- The smooth constraint: to ensure a smooth surface.
- The integrability constraint: to ensure a valid integrable surface.
- The intensity gradient constraint: to ensure that the intensity gradient of the reconstructed image is close to the intensity gradient of the input image.
- The unit normal constraint: to force the recovered surface normal to be unit vector.

In this paper, we introduce two constraints, the smooth constraint and integrability constraint, for the SFS scheme.

1) *The Smooth Term:* We take the smoothness constraint [Zha99]:

$$\psi(n, N) = \left\| \frac{\partial n}{\partial x} \right\|^2 + \left\| \frac{\partial n}{\partial y} \right\|^2 \quad (3)$$

where N means the neighborhood around the normal n . The 4-neighborhood smooth constraint is chosen in our scheme. In the discrete grid of coordinates, the updated surface normal at $(k + 1)^{th}$ iteration is estimated by the value at k^{th} iteration as

$$n_{i,j}^{k+1} = \bar{n}_{i,j}^k \quad (4)$$

where $\bar{n}_{i,j}^k$ is the mean of the 4-neighborhood surface normal around (i, j) . However, one of the most serious disadvantages of this smooth term is it quickly leads to a flat surface and results in poor

surface recovery. Therefore, we use a simple Gaussian filter to perform preprocessing first:

$$G(s, t) = \frac{1}{2\pi\sigma^2} \exp\left(-\frac{s^2 + t^2}{2\sigma^2}\right) \quad (5)$$

where σ is a constant, which is taken as 0.6 in our experiments and $s, t = 1, 0, 1$. Thus for a 3x3 neighborhood the new equation is:

$$\bar{n}_{i,j} = \sum_{s=-1}^1 \sum_{t=-1}^1 G(s, t) \times n_{i+s, j+t} \quad (6)$$

2) *The Integrability Term:* Frankot and Chellappa's algorithm [Fra88] introduced the integrability constraint into the energy function to recover valid surfaces, that is, $Z_{xy} = Z_{yx}$. The integrability term can be described as:

$$\iint (Z_{xy} - Z_{yx})^2 dx dy \quad (7)$$

Inspired by their works, we introduce the integrability regular term in geometry:

$$\tau(n, N) = (Z_{xy} - Z_{yx})^2 = (e_2 \frac{\partial n}{\partial x} - e_1 \frac{\partial n}{\partial y})^2 \quad (8)$$

where e_1 and e_2 are unitary, that is, $e_1 = (1, 0, 0)$ and $e_2 = (0, 1, 0)$. Here $e_1 \frac{\partial n}{\partial y}$ and $e_2 \frac{\partial n}{\partial x}$ are dot products. To discretize $\tau(n, N)$ directly, we can gain the following equation:

$$\tau(n_{i,j}, N_{i,j}) = \frac{1}{2} (e_2(n_{i+1,j} - n_{i,j}) - e_1(n_{i,j+1} - n_{i,j}))^2 + \frac{1}{2} (e_2(n_{i,j} - n_{i-1,j}) - e_1(n_{i,j} - n_{i,j-1}))^2 \quad (9)$$

Applying the calculus of $n_{i,j}$ yields the following iterative operation:

$$\begin{cases} \tilde{n}(1)_{i,j} = (n(1)_{i,j+1} + n(1)_{i,j-1}) / 2 \\ \tilde{n}(2)_{i,j} = (n(1)_{i+1,j} + n(1)_{i-1,j}) / 2 \\ \tilde{n}(3)_{i,j} = n(3)_{i,j} \end{cases}$$

where $n(x) \dots$ is the x^{th} component ($x=1,2,3$) of the normal $n \dots$, and $\tilde{n}(\dots)$ means the value of parenthesized component after this integral operation.

Actually, the integrability term plays a role in substituting the first component of the target normal with the mean of the first components of the up-down normal in the 4-neighborhood, and substituting the second component of the target normal with the mean of second components of the left-right normal. This improvement changes the surface normal gradually in iterations, and provides a more accurate recovered surface in the following experiment.

C. Normal Rotation

After regular operation, the surface normal may fall off the reflect cone. So they need to rotate back to the cone. The axis of this rotation is given by the cross product between the fall-off surface normal $\bar{n}_{i,j}^k$ and light S :

$$(u, v, w)' = \bar{n}_{i,j}^k \times S$$

The rotation axis is perpendicular to both the light direction S and the off-cone normal $\bar{n}_{i,j}^k$. The angle of this rotation is equal to:

$$\theta = \arccos E - \arccos \frac{\|\bar{n}_{i,j}^k\|}{\|\bar{n}_{i,j}^k\| \|S\|}$$

Hence, the rotation matrix is:

$$\Theta = \begin{pmatrix} c + u^2 c' & -ws + uvc' & vs + uwc' \\ ws + uvc' & c + v^2 c' & -us + vwc' \\ -vs + uwc' & us + vwc' & c + w^2 c' \end{pmatrix} \quad (10)$$

where $c = \cos \theta$, $c' = 1 - c$, $s = \sin \theta$. The off-cone normal is rotated to the cone by Θ .

D. Framework of the Proposed SFS Algorithm

Summarizing the above derivation, our SFS algorithm can be represented by the following steps:

- 1) Initialize the surface normal field N^0 with the intensity gradient.
- 2) Smooth the surface normal field with the smooth regular term $n_{i,j}^{k+1} = \psi(n_{k,j}^k, N_{k,j}^k)$ according to equation (3).
- 3) Enforce integrability using the integrability regular term $n_{i,j}^{k+1} = \tau(n_{k,j}^k, N_{k,j}^k)$ according to equation (8).
- 4) Rotate the normal to satisfy the brightness constraint $n_{i,j}^{k+1} = \Theta(n_{k,j}^k)$ according to equation (10).
- 5) Normalize the normal.
- 6) If it converges, terminate the iteration, otherwise go back to step 2.

3. FACE RECOGNITION STRATEGIES

Lots of features can be exploited in 3D surface matching [Zha00b,Wu04,Pan05]. The surface curvature is one of the most important. In this section we explore the ability of three different face recognition strategies by using surface normal fields obtained from the above SFS algorithm. The strategies are respectively dot product based, curvedness histograms based, and shape index based strategy.

A. Dot Product based Strategy

Dot product is the most straightforward operation. It measures the similarity of two normal fields N and M directly by computing the dot product. The smaller the dot product is, the more similar these two fields are. The distance between two normal fields is defined as:

$$d_{dp} = \sqrt{\sum_{i,j} (1 - N_{i,j} \cdot M_{i,j})^2} \quad (11)$$

where N and M are the unit normal fields of two surfaces. Dot product distance d_{dp} measures the difference of surface normal in each pixel. However, its recognition ability is not good because the normal field is affected by the image noise and the error introduced in the estimation of the light direction.

B. Curvedness Histograms based Strategy

The curvedness histogram idea enhances the fact that though the SFS algorithm fails to obtain an accurate surface, the recovered surface in essence is the same as the original one. Therefore, it is a good choice to apply curvedness to measure the similarity of two surfaces extracted from the SFS algorithm. Usually, the surface curvedness can be computed from the Hessian matrix:

$$H = \begin{pmatrix} \left(\frac{\partial n}{\partial x} \right)_x & \left(\frac{\partial n}{\partial x} \right)_y \\ \left(\frac{\partial n}{\partial y} \right)_x & \left(\frac{\partial n}{\partial y} \right)_y \end{pmatrix} \quad (12)$$

where $(\dots)_x$ and $(\dots)_y$ are the x and y components of the parenthesized vectors respectively. From this matrix, the most important attributes are these curvatures \mathcal{K}_1 and \mathcal{K}_2 , which are the eigenvalues of the Hessian matrix. With the principal curvatures, several local surface attributes can be defined:

- Mean curvature: The mean curvature K is the mean of the principal curvatures:

$$K = \frac{1}{2}(\kappa_1 + \kappa_2).$$

- Gaussian curvature: The Gaussian curvature G is the product of the principal curvatures: $G = \kappa_1 \kappa_2$.
- Curvedness: The curvedness C is another measure derived from the principal curvatures: $C = \frac{1}{2}\sqrt{\kappa_1^2 + \kappa_2^2}$.
- Shape Index: The shape index labels the type of shape using the principal curvatures in angular measure as: .

$$\phi = \frac{2}{\pi} \arctan \frac{\kappa_2 + \kappa_1}{\kappa_2 - \kappa_1} \quad \kappa_2 \geq \kappa_1 \quad (16)$$

Detailed discussion will be given in the following subsection.

In practice, we prefer curvedness of 2-D histogram to 1-D. This 2-D histogram with $m \times n$ bins is built by counting the curvedness in each bin. Then Euclidean distance is simply adopted to compare two histograms as follows:

$$d_{hist} = \sqrt{\sum_{i=1}^m \sum_{j=1}^n (HM_{i,j} - HN_{i,j})^2} \quad (17)$$

where HM and HN denote two histograms with $m \times n$ bins.

C. Shape Index based Strategy

Shape index is a high-level characteristic extracted from the surface normal field. It can be computed from the principal curvatures mentioned above. Usually, shape index is used to label local surface shapes according to the following table [Wor01]:

Region type	Shape index	Weight
Cup	$(-1, -5/8]$	-3
Rut	$(-5/8, -3/8]$	-2
Saddle rut	$(-3/8, -1/8]$	-1
Saddle point	$(-1/8, 1/8]$	0
Plane		Null
Saddle ridge	$(1/8, 3/8]$	1
Ridge	$(3/8, 5/8]$	2
Dome	$(5/8, 1]$	3

Table 1. Topographic Labels

These seven region type labels are set with different weights. After the surface is labeled, label vector (LV) needs computing:

$$LV = (LV_1, LV_2, \dots, LV_7) \quad (18)$$

where LV denotes the label vector, and its component LV_i represents number of i^{th} label on the surface. Actually, LV represents the statistical information of shape index in the surface.

Then the LV is sorted with ascending order. From the sorted label vector (SLV), we can obtain the number of each label and the main label in the surface, which is the last component in the SLV . According to this analysis, shape index based difference can be measured:

$$d_{shi} = \sum_1^7 (SLVA_i - SLVB_i)^2 \exp(\|weight(SLVA) - weight(SLVB)\|) \quad (19)$$

where $SLVA$ and $SLVB$ are two sorted label vectors, and $weight(\cdot)$ is the cost function which returns the weight of the parenthesized components.

4. EXPERIMENTS

The experiments consist of two parts: geometric-based SFS algorithm with integrability regular term and face recognition SFS. We commence by evaluating the performance of this improved SFS algorithm with synthetic images. The second part will focus on face recognition with three different strategies using surface normal fields obtained from the above SFS and evaluates its ability for face recognition in the varying light situation.

A. Shape from Shading

In this part, we generate the synthetic ball image to test our SFS algorithm. The ball is created using the following formula:

$$Z(x, y) = \sqrt{2500 - x^2 - y^2}$$

where $-50 \leq x, y \leq 50$, and $x^2 + y^2 \leq 2500$. This yields a true half sphere with radius 50. Using the Lambertian assumption, the reconstructed picture with the light direction $S = (0; 0; 1)$ can be generated in Fig. 1. Then, we obtain the 3D information of the sphere by applying the proposed algorithm in Fig. 2. As benchmark, results based on Worthington and Hancock's are listed in the second column. Fig. 2 shows the normal field, curvedness histogram and shape index label of the original sphere and the results recovered by Worthington and Hancock's and our algorithm respectively. Comparing their SFS method and our method, we find that there is a small difference just from the surface normal fields, but our algorithm achieves a better improvement by

curvedness histogram and shape index label. In Table 2, errors of recovered results by Worthington and Hancock's and our algorithms are shown respectively. Obviously, the error in our algorithm is much smaller than theirs, especially for d_{cur} and d_{shi} .

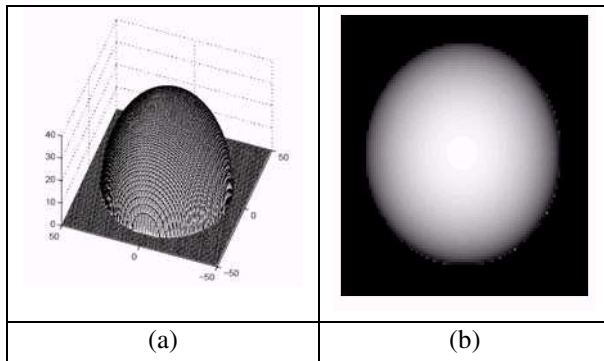


Figure 1. Synthetic sphere: (a) the true height map of the ball, (b) the reconstructed image with light direction $S = (0, 0, 1)$

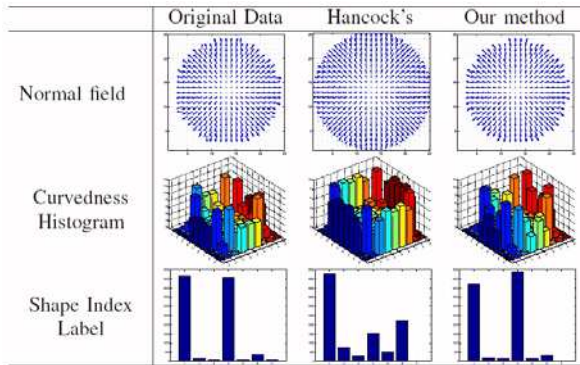


Figure 2. Comparison between original data and the recovered results of Worthington and Hancock's [Wor01] and ours respectively.

Algorithms	d_{dp}	d_{cuv}	d_{shi}
Worthington and Hancock	94.4	34.8	7228
Ours	66.7	15.2	2244

Table 2. Error comparison between Worthington and Hancock's [Wor01] and ours

B. Face Recognition

In order to investigate the recognition ability of the proposed method in face recognition, we conducted experiments with three different strategies described in this section. The database adopted in our experiment is the not-lighted group of the CMU illumination pie database, which consists of 1428 pictures (21 illuminations of 68 persons). All of these images have been aligned in advance. Here we use 4

kinds of different testing sets: Set5, Set10, Set15, Set18. "Seti" means i types out of 21 illumination conditions for each person, which are chosen randomly as the testing set, and the rest of pictures are used as the training set. Fig. 3 is a subset of Set5. Fig. 4 gives the midway results which show the human face's normal field, curvedness histogram and shape index for 2 persons under different illumination conditions. From this figure, we can find that the same person has similar features including normal field, curvedness histogram and shape index label from the proposed algorithm.

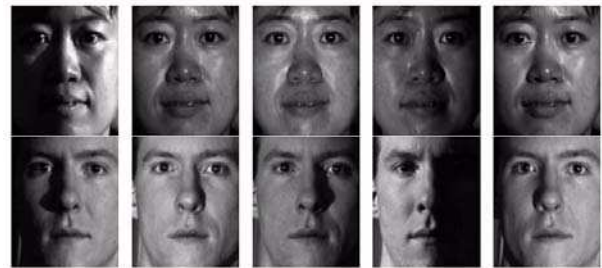


Figure 3. Example of face images used in our experiment. Each row includes pictures of the same person in different light directions.

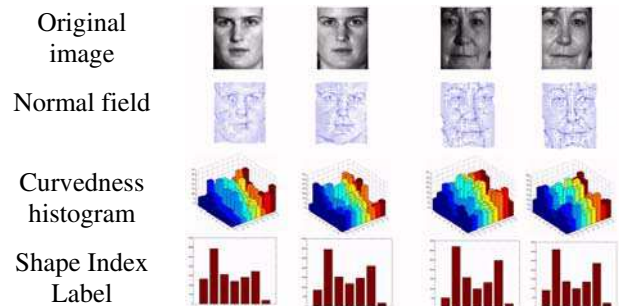


Figure 4. The feature representation for two human face images under different illuminations

In the face recognition stage, all experiments are repeated randomly for 20 times and the recognition rate is taken as the average of all 20 times. The recognition rates and standard deviation are presented in Table 3. Dot product based strategy (d_{dp}) performs rather poorly in Set18 and Set15. Scores for Strategies for curvedness histogram based (d_{cuv}) and shape index based (d_{shi}) are very close, both produced a much higher performance. In Set5, they achieve a recognition rate of 96%. To evaluate our method, we choose a typical face recognition method PCA+LDA as benchmark to carry out further experiments using the same database [Tur91, Bel97]. A comparison between PCA+LDA and the proposed is displayed in Fig 5. The results show that the

recognition rate of the proposed method has achieved about 5% higher than that of PCA+LDA in all testing sets. These results demonstrate that the proposed method perform well in the recovery and representation of 3D objects and recognition.

	Set 18	Set 15	Set 10	Set 5
d_{dp}	47.2±12	52.7±16	75.6±8	81.2±9
d_{cuv}	79.3±27	83.8±22	94.1±8	96.1±8
d_{shi}	79.2±27	83.7±22	94.0±8	96.0±8

Table 3. Recognition Rate for 3 strategies and 4 sets

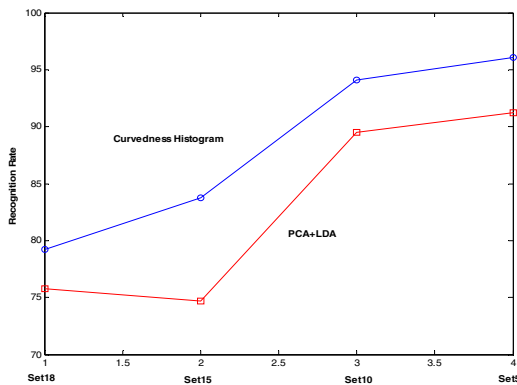


Figure 5. Comparison between typical PCA+LDA and the proposed method.

5. CONCLUSION

In this paper, we explored face recognition using surface normal fields derived from SFS. The investigation consists of two aspects. First, the integrability regular term is introduced into Worthington and Hancock's geometric-based SFS algorithm and it leads to a much more accurate reconstructed surface normal field. Second, we use three different strategies for face recognition in testing the ability to handle light variations. We find that curvedness histogram and shape index based strategies perform much better than the dot product. Furthermore, compared with typical face recognition by PCA+LDA, the proposed method has demonstrated its ability in overcoming illumination variations because the features derived from surface local topological information are more robust under light variations.

REFERENCES

- [Bel97] P. N. Belhumeur, J. P. Hespanha and D. J. Kriegman, "Eigenface vs Fisherfaces: Recognition Using Class Specific Linear Projection," *IEEE Trans. on PAMI*, Vol. 20, No. 7, pp. 711-720, 1997
- [Bic92] M. Bichsel and A. P. Pentland, "A Simple Algorithm for Shape from Shading," *IEEE Proc. Computer Vision and Pattern Recognition*, pp. 459-468, 1992
- [Fra88] R. T. Frankot and R. Chellappa, "A Method for Enforcing Integrability in Shape from Shading Algorithms," *IEEE Trans. PAMI*, Vol. 10, No. 4, pp. 439-451, 1988
- [Geo01] A. S. Georghiades, P. N. Bellhumeur, and D. J. Kriegman, "From Few to Many: Illumination Cone models for Face Recognition under Pose and Lighting," *IEEE Trans. on PAMI*, Vol. 23, No. 6, pp. 643-660, 2001
- [Hor70] B. K. P. Horn, "A Method for Obtaining the Shape of a Smooth Opaque Object from One View," *PhD thesis*, MIT, 1970
- [Hor81] B. K. P. Horn and M. J. Brooks, "Shape and Source from Shading," *Int. Joint Conf. on Artificial Intelligence*, pp. 932-936, Los Angeles, 1985
- [Ike81] K. Ikeuchi and B. K. P. Horn, "Numerical Shape from Shading and Occluding Boundaries," *Artificial Intelligence*. Vol. 17, No. 1-3, pp. 141-184, 1981
- [Lee85] C. H. Lee and A. Rosenfeld, "Improved Methods of Estimating Shape from Shading Using the Light Source Coordinate System," *Artificial Intelligence*, Vol. 23, No. 2, pp. 125-143, 1985
- [Liu06] L. Y. Liu, S. G. Shan, X. L. Chen and W. Gao, "Face Recognition Varying Light Based the Harmonic Images," *Chinese Journal of Computers*, Vol. 29, No. 5, pp. 760-768, 2006
- [Mog00] B. Moghaddam, T. Jebara and A. Pentland, "Bayesian Face Recognition," *Pattern Recognition*, Vol. 33, No. 11, pp. 1771-1782, 2000
- [Pan05] G. Pan, S. Han, Z. H. Wu and Y. M. Wang, "3D Face Recognition Using Mapped Depth Images," *CVPR'2005*, pp.1-7, 2005
- [Phi00] P. J. Phillips, H. Moon, S. A. Rizvi *et al.*, "The RERET Evaluation Methodology for Face Recognition Algorithms," *IEEE Trans. on PAMI*, Vol. 22, No. 10, pp. 1090-1104, 2000

- [Phi03] P. J. Phillips, P. Grother, R. J. Macheals, *et al.*, "FRVT 2002: Evaluation Report," http://www.frvt.org/DLs/FRVT_2002_Evaluation_Report.pdf, March, 2003.
- [Pra03] E. Prados and O. Faugeras, "A Mathematical and Algorithmic Study of the Lambertian SFS Problem for Orthographic and Pinhole Cameras," *INRIA Report*, 2003
- [Rou92] E. Rouy and A. Tourin, "A Viscosity Solutions Approach to Shape-from-Shading," *SIAM Journal on Numerical Analysis*, Vol. 29, No. 3, pp. 867-884, 1992
- [Sha01] A. ShaShua and T. Riklin-Raviv, "The Quotient Image: Class-based Re-rendering and Recognition with Varying Illuminations," *IEEE Trans. on PAMI*, Vol. 23, No. 2, pp. 129-139, 2001.
- [Tsa94] P. S. Tsai and M. Shah, "Shape from Shading Using Linear Approximation," *Image and Vision Computing*, Vol. 12, No. 8, pp. 487-498, 1994
- [Tur91] M. Turk and A. Pentland, "Eigenfaces for Recognition," *Journal of Cognitive Neuroscience*, Vol. 3, No. 1, pp. 71-86, 1991
- [Wor99] P. L. Worthington and E. R. Hancock, "New Constraints on Data-Closeness and Needle Map Consistency for Shape-from-Shading," *IEEE Trans. on PAMI*, Vol. 21, No. 12, pp. 1250-1267, 1999
- [Wor01] P. L. Worthington and E. R. Hancock, "Object Recognition Using Shape-from-Shading," *IEEE Trans on PAMI*, Vol. 23, No. 5, pp. 535-542, 2001
- [Wu04] Z. H. Wu, Y. M. Wang and G. Pan, "3D Face Recognition Using Local Shape Map," *ICIP'2004*, pp. 2003-2006, 2004,
- [Zha99] R. Zhang, P. S. Tsai, J. E. Cryer and M. Shah, "Shape from Shading: a Survey", *IEEE Trans. on PAMI*, Vol. 21, No. 8, 1999
- [Zha00a] W. Y. Zhao and R. Chellappa, "Illumination-Insensitive Face Recognition Using Symmetric Shape-from-Shading," *CVPR'2000*, pp. 286-293, 2000
- [Zha00b] W. Y. Zhao and R. Chellappa, "SFS Based View Synthesis for Robust Face Recognition," *AFGR'2000*, pp. 285-292, 2000
- [Zha03] W. Y. Zhao, R. Chellappa, A. Rosenfeld and P. J. Phillips, "Face Recognition: a Literature Survey," *ACM Computing Survey*, Vol. 35, No. 4, pp. 399-458, 2003
- [Zhe91] Q. Zheng and R. Chellappa, "Estimation of Illumination Direction, Albedo, and Shape from Shading," *IEEE Trans. on PAMI*, Vol. 13, No. 7, pp. 680-702, 1991